Journal of Solid State Chemistry **159,** 336–342 (2001)
doi:10.1006/jssc.2001.9177, available online at http://www.idealibrary.com on IDEAL®

Photo- and Dehydration-Induced Charge Transfer Processes Accompanied with Spin Transition on $CoFe(CN)_5NH_3 \cdot 6H_2O$

Z.-Z. Gu,* Y. Einaga,† O. Sato,* A. Fujishima,† and K. Hashimoto‡,[1]

*Kanagawa Academy of Science and Technology, KSP Bldg. East 412, 3-2-1 Sakado, Takatsu-ku, Kawasaki-shi, Kanagawa 213-0012, Japan; †Department of Applied Chemistry, University of Tokyo, 7-3-1 Hongo Bunkyo-Ku, Tokyo 113-8565, Japan; and ‡Research Center for Advanced Science and Technology, University of Tokyo, 4-6-1 Komaba, Meguro-ku, Tokyo 153-8904, Japan

Received March 20, 2001; accepted March 21, 2001

IN DEDICATION TO THE LATE PROFESSOR OLIVIER KAHN FOR HIS PIONEERING CONTRIBUTIONS TO THE FIELD OF MOLECULE MAGNETISM

The coexistence of different valences of iron and cobalt in cobalt pentacyanoferrate, $CoFe(CN)_5NH_3 \cdot 6H_2O$, was confirmed by the infrared spectrum, in which two distinct peaks for the C–N stretch at 2162 cm^{-1} and 2117 cm^{-1} were assigned to CN in Fe^{III}–CN–Co^{II} and Fe^{II}–CN–Co^{III} respectively, and by the Mössbauer spectrum, in which Fe^{III} and Fe^{II} exhibited doublets with different isomer shifts and different quadrupole splitting. Photo-irradiation of this compound with red light changed the population of these two electronic states due to the internal electron transfer from Fe^{II} to Co^{III}. As a result, the ferrimagnetic properties of this pentacyanometalate at low temperature can be changed by photo-irradiation similar to the case of the hexacyanometalate, $K_{0.2}Co_{1.4}Fe(CN)_6 \cdot 6.9H_2O$ reported previously (O. Sato *et al., Science* 272, 704 (1996)). Moreover, the fraction of these two electronic states in this pentacyanoferrate is sensitive to the number of water molecules, which induces a charge transfer from Co^{II} and Fe^{III}. As a result, dehydration increases the fraction of Fe^{II}–CN–Co^{III} and causes the compound to be paramagnetic even at low temperature.

INTRODUCTION

Although the field of molecule-based magnets started only about 13 years ago, it has, in that time, attracted a broad spectrum of researchers (1–4). The optical and magnetic properties of Prussian blue analogues, which are composed of transition metal ions and hexacyanometalates, have been studied extensively (3, 5–12). In these compounds, various types of metal ions are bridged by the cyanide ligands to form a three-dimensional structure containing interstitial ions and water molecules. One of the most interesting compounds in this family is $A_xCo_y[Fe(CN)_6] \cdot xH_2O$, which shows photo-induced magnetization. Many experimental and theoretical studies have been performed on this family of compounds to date (13–25).

A family of cyanide compounds related to the hexacyanometalate group is that of molecules consisting of a substituted pentacyanometalate moiety, $[Fe(CN)_5L]^{n-}$, (L = NO, NH_3, H_2O, SO_4^{2-}, or pseudohalide), which also form extended cross-linked structures (26). Powder X-ray diffraction (XRD) analysis of these pentacyano compounds reveals a face-centered cubic (fcc) pattern similar to that of the hexacyano compounds. Since the symmetry group of $[Fe(CN)_5L]^{n-}$ is not O_h, the fcc structure indicated by powder XRD is usually explained by local disorder of the ligand L (26, 27). There have been several reports in the literature regarding the structures of $M[Fe(CN)_5NO] \cdot xH_2O$ compounds (M = Mn, Fe, Co, Zn, Cd) based on single-crystal XRD data (28–31). In these compounds, Fe is coordinated by five cyanides on the C side and one nitrosyl ligand, and the other metal, M, is coordinated to five cyanides on the N side and one water molecule. The cyanide ion serves to link the metal cations to form a dense three-dimensional network, but because they are only coordinated to a single metal center, the NO ligands and bound water molecules allow for the formation of open channels.

For molecule-based magnets, the solvent molecules typically play an important role in the electronic states (32–37). Dehydration is always accompanied by a dramatic change in the physical properties, which is especially apparent for the polycyanide compounds. A color change from pink to blue by dehydration was observed for $Co[Co(CN)_6] \cdot xH_2O$ (38). This is explained by a decrease in the number of water ligands associated with the interstitial cobalt ions. Such a dehydration-induced color change was also observed for the compound produced from cobalt pentacyanonitrosylferrate and nickel pentacyanonitrosylferrate (39), although interstitial ions do not exist in this case.

In this paper, we report on a new compound, namely cobalt pentacyanoammineferrate, without interstitial ions,

[1] To whom correspondence should be addressed.

0022-4596/01 $35.00

whose color as well as structure and magnetic properties, can be changed greatly by dehydration or photo-irradiation.

EXPERIMENTAL

Sodium pentacyanoammineferrate (Wako Chemicals) was purified in 28% ammonia solution (Wako). It was prepared according to the method described in the literature (40–42). Cobalt pentacyanoammineferrate was synthesized by adding a 0.8 M aqueous solution of cobalt(II) sulfate (Wako) to a 0.8 M aqueous solution of sodium pentacyanoammineferrate. The precipitate ($CoFe(CN)_5NH_3 \cdot 6H_2O$) was collected by filtration and dried in air. [Anal.: Fe, 15.1%; Co, 15.9%; C, 16.2%; N, 22.7%; H, 4.1%. Found: Fe, 14.8%; Co, 16.0%; C, 16.2%; N, 22.6%; H, 4.0%.]

Infrared (IR) and ultraviolet (UV)-visible light spectral measurements were performed either at room temperature or at 18 K. A closed-cycle helium refrigerator (Iwatani Plantech Corp.) was used to control the temperature. IR spectra were obtained on a Bio-RAD spectrophotometer. The experimental error was less than 1 cm^{-1}. The sample was held between CaF_2 plates. UV-visible spectra were recorded on a Shimadzu model UV-3100PC spectrophotometer. Powder XRD was performed at room temperature. Thermal gravimetric analysis (TGA) and differential thermal analysis (DTA) were performed simultaneously by increasing the temperature at a constant rate (2 K/min). The Mössbauer spectra were measured with a Wissel model MVT-1000 Mössbauer spectrometer with a $^{57}Co/Rh$ source in the transmission mode. Magnetic susceptibilities were measured with a superconducting quantum interference device (SQUID) magnetometer (Quantum Design). An Hg–Xe lamp was used as the light source, and a sharp cut-off filter was used to obtain light of wavelengths between 620 and 750 nm. The red light was guided by an optical fiber to irradiate the sample in the refrigerator and in the SQUID. The light intensity was $\sim 2\ mW/cm^2$ and the irradiation time was 1 h.

RESULT AND DISCUSSION

Structure, Electronic State, and Magnetic Properties

The powder XRD patterns show that $CoFe(CN)_5NH_3 \cdot 6H_2O$ is crystallized in a fcc form, which is typical for compounds composed of hexacyanometalates and pentacyanometalates (27, 30, 43, 44). The lattice constant was determined to be 10.20 Å. For the compound prepared from cobalt pentacyanonitrosylferrate (30), single-crystal XRD shows that every iron is coordinated by five CN ligands (C side) and one NO and every cobalt is coordinated to five CN ligands (N side) and one water molecule. The cyanide ligands link iron and cobalt cations to form a three-dimensional network. Such a coordination can also be used to explain the environment of the metal ceners in $CoFe(CN)_5NH_3 \cdot 6H_2O$ (Fig. 1). As the symmetry of pentacyanoferrate is C_{4v}, the fcc structure indicated by powder XRD is considered to be due to local disorder of the NH_3 ligands and coordinated water molecules (30, 45).

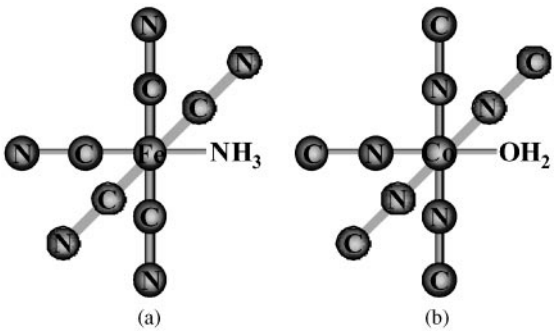

FIG. 1. Coordination structures of (a) iron- and (b) cobalt-containing moieties in cobalt pentacyanoammineferrate.

The IR spectrum shows two peaks for the C–N stretch, ν(CN), at 2117 and 2162 cm^{-1} (Fig. 2a). The 2162 cm^{-1} peak is assigned to CN in Fe^{III}–CN–Co^{II} (46). This appears at a higher wavenumber than it does in $Na_2Fe^{III}(CN)_5NH_3 \cdot H_2O$ ($\sim$ 2119 cm^{-1}). Such a blue shift is usually observed in the bridging mode for Prussian blue analogues. The 2117 cm^{-1} peak is somewhat unusual, because it appears at a wavenumber lower than that of the aforementioned sodium compound. This type of unusual red shift was also observed in the cobalt polycyanides, $Na_xCo_{1.3}Fe(CN)_6 \cdot yH_2O$ and $K_{0.2}Co_{1.4}[Fe(CN)_6] \cdot 6.9H_2O$, which was explained in terms of the appearance of Fe^{II}–CN–Co^{III} after

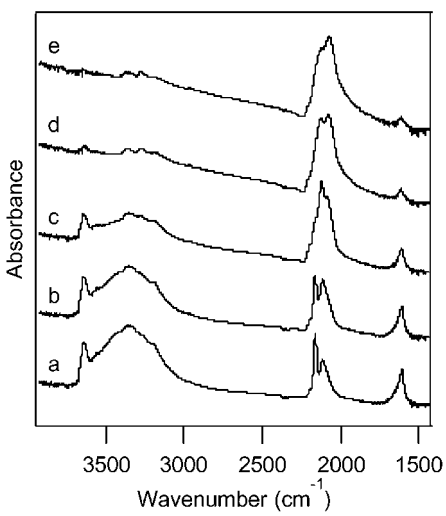

FIG. 2. IR spectra of $CoFe(CN)_5NH_3 \cdot 6H_2O$ observed at (a) 298, (b) 313, (c) 333, (d) 363, and (e) 383 K.

the cross-linking reaction (9). Therefore, the IR spectrum suggests the coexistence of Fe^{III}–CN–Co^{II} and Fe^{II}–CN–Co^{III} sites in the compound examined in the present work.

Figure 3 depicts the Mössbauer spectrum of this compound at room temperature, in which two pairs of doublets are observed. The isomer shift (IS) for the small inner doublet is -0.09 mm/s, and the quadruple splitting (QS) is 0.74 mm/s. The isomer shift for the outer doublets is -0.17 mm/s and its quadrupole splitting is 1.74 mm/s. The IS is related to the charge density and the spin state of an atom, while the QS gives information on the gradient of the electric field around the atom. Therefore, comparison of the measured data with those of related compounds makes it possible to determine the valence of the atom. For the mononuclear compounds of the type $[Fe^{II}(CN)_5L]^{3-}$, the IS values ranges from 0.00 to 0.04 mm/s, and the QS values from $\sim$0.26 to $\sim$0.29 mm/s (47, 48). In contrast, compounds of the type $[Fe^{III}(CN)_5L]^{2-}$ are in the range -0.15 to -0.06 mm/s and from 0.91 to 2.54 mm/s for IS and QS, respectively. Therefore, the inner and outer doublets of the present compound can be assigned to Fe^{II} and Fe^{III}, respectively. This assignment is also supported by the observation of magnetic splitting below 10 K (49). Magnetic relaxation was observed in the outer doublet, while no relaxation was observed in the inner doublet at this temperature. A fitting of the Mössbauer spectrum shows that the ratio of Fe(III):Fe(II) in this compound is 3:1.

Curve (a) in Fig. 4 represents the field-cooled magnetization (FCM) measured in an external field of 5 G, which reveals an abrupt break at $\sim$11 K. The paramagnetic susceptibility (χ) obeyed the Curie–Weiss law, $\chi = C/(T-\theta)$, in the temperature region from 270 to 50 K, with a Curie constant, $C = 3.6\ \mathrm{cm^3/mol}$, and a negative Weiss constant, $\theta = -8.3$ K, indicative of the existence of an antiferromagnetic interaction between Fe^{III} and Co^{II}. The antiferromagnetic interaction was also indicated in the χ–T plot, which shows a minimum at $\sim$80 K. The μ_{eff} at 280 K is about 5.2 μ_B. This value is larger than the theoretical one, 4.2 μ_B, in which only the spin contribution at the high-temperature limit for Fe^{III}–CN–Co^{II} is considered. This corresponds to the sum of local contributions from the cobalt and iron sites, $\mu_{eff} = \{\gamma[g_{Fe}^2 S_{Fe}(S_{Fe}+1) + g_{Co}^2 S_{Co}(S_{Co}+1)]\}^{0.5}$, where the local Zeeman factors, g_{Co} and g_{Fe} are assumed to be 2, $S_{Co} = \frac{3}{2}$ and $S_{Fe} = 1$ are the local spin number for Fe^{III} and Co^{II}, and $\gamma = 0.67$ is the ratio of Fe^{III}–CN–Co^{II} to Fe^{II}–CN–Co^{III} derived from the results of the Mössbauer spectrum. Such a large μ_{eff} may be ascribed to the very large experimental value of g_{Co}, which can always be observed for the high-spin Co^{II} (50).

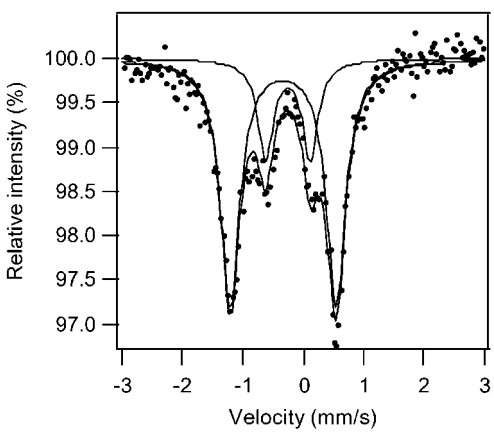

FIG. 3. Mössbauer spectrum of $CoFe(CN)_5NH_3 \cdot 6H_2O$ at room temperature.

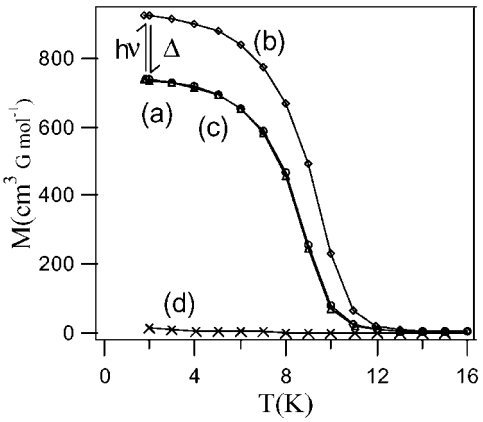

FIG. 4. Field-cooled magnetization vs temperature of $CoFe(CN)_5NH_3 \cdot 6H_2O$ observed at an external field of 5 G: (a) before irradiation (●), (b) after irradiation (◆), (c) recovered by raising the temperature to 150 K (▲); and (d) after dehydration at 337 K (*).

Photoirradiation Effect

The UV-visible absorption spectrum of this compound shows a broad absorption (Fig. 5). By analogy with the Co–Fe hexacyanometalate (9), the shoulder at $\sim$500 nm can be assigned to the charge transfer (CT) band from Fe^{II} to Co^{III}. This assignment is confirmed by recent theoretical calculations (25, 51). The excitation of this transition with red light at 18 K changes the IR spectrum, as shown in Fig. 6. The 2117 cm^{-1} band (Fe^{II}–CN–Co^{III}) decreased and the 2162 cm^{-1} band (Fe^{III}–CN–Co^{II}) increased, suggesting that an electron is transferred from Fe^{II} to Co^{III}. An important point is that this spectral change was maintained at low temperature even after stopping the irradiation, indicating the formation of a metastable state. By increasing the temperature above 150 K, the spectrum reverted to that observed before irradiation.

The field-cooled magnetization (FCM) vs temperature after irradiation is shown in Fig. 4. The magnetization increased by about 25% at 2 K, measured at an external

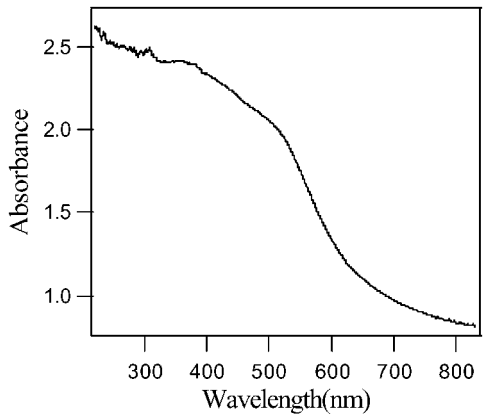

FIG. 5. Diffuse reflectance UV-visible spectrum of $CoFe(CN)_5NH_3 \cdot 6H_2O$ at room temperature.

field of 5 G. By increasing the temperature above 150 K, the FCM curve reverted to the initial one (curve c). These changes in the magnetic properties are very similar to those observed for $K_{0.2}Co_{1.4}[Fe(CN)_6] \cdot 6.9H_2O$ and are explained by an increase of the fraction of the Fe^{III}–CN–Co^{II} configuration.

At low temperature, the spins align through the Fe^{III}–CN–Co^{II} sites in the three-dimensional network. Therefore, the increases in the magnetization and T_c are due primarily to an increase in the number of aligned spins and the number of exchange coupling pathways. The changes in the magnetization response after irradiation was also observed in the hysteresis. The change at 5 K is shown in Fig. 7. Before irradiation, the coercive force is 846 G and the residual magnetization is 3.491×10^3 $cm^3\,G\,mol^{-1}$, which are increased to 991 G and 3994 $cm^3\,G\,mol^{-1}$ respectively by irradiation.

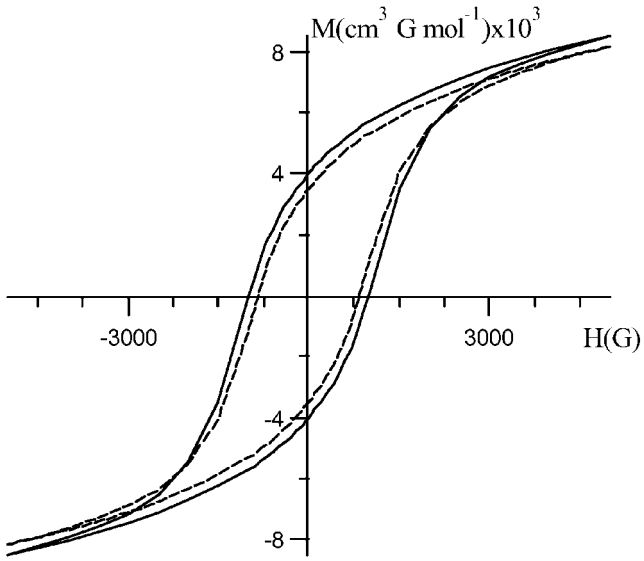

FIG. 7. Field dependence of magnetization at 2 K before (dashed line) and after (solid line) irradiation.

Dehydration-Induced Changes

In general, water molecules contained in Prussian blue analogues are removed by heating. The loss of water upon heating was observed by TGA (Fig. 8), which shows a continuous decrease in weight as the temperature rises from 298 to 381 K. The compound loses ~ 5 water molecules per $CoFe(CN)_5NH_3 \cdot 6H_2O$ unit in this temperature range. This result shows that two types of water molecules, each with a different bonding energy, exist in this compound. The water molecules lost below 381 K have a small bonding energy and can be regarded as those that are not bonded to

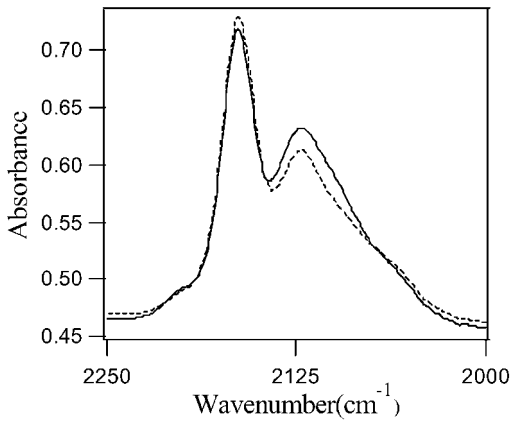

FIG. 6. IR spectrum of $CoFe(CN)_5NH_3 \cdot 6H_2O$ at 18 K. The solid line is the spectrum before irradiation. The dashed line is that obtained after irradiation for 20 min.

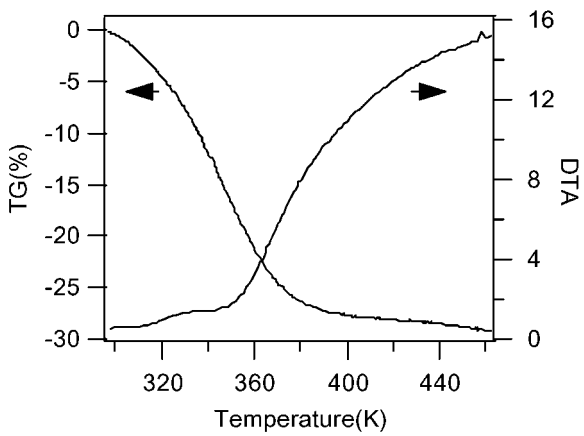

FIG. 8. Thermal gravimetric analysis (TGA) and differential thermal analysis (DTA) curves for $CoFe(CN)_5NH_3 \cdot 6H_2O$.

the metal cations. Conversely, the water molecules with a larger bonding energy may be bonded directly to the cobalt. The number of such bound water molecules estimated from TGA is ~ 1 per $CoFe(CN)_5NH_3 \cdot 6H_2O$ unit, which is consistent with a structure in which one water molecule coordinates to a cobalt ion. The DTA curve, which is also shown in Fig. 8, exhibits an exothermic transition at about 340 K. The number of water molecules lost at this temperature is 3 per $CoFe(CN)_5NH_3 \cdot 6H_2O$ unit.

The XRD pattern showed that dehydration induces a change in the crystal structure. All the samples are predehydrated at a definite temperature and then cooled to room temperature for measurement. Dehydration at temperatures below 340 K decreased the lattice constant from 10.20 Å (room temperature) to 9.93 Å (340 K). Above this temperature, an apparent line broadening and a decrease in the number of diffraction peaks were observed, and the peaks characteristic of the fcc structure gradually disappeared with increasing temperature. These observations indicate that the transition observed by DTA at ~ 340 K is due to a structural transition from fcc to amorphous.

The IR spectra of this compound at various temperatures are shown in Fig. 2. The sharp peaks at 3640 and 3362 cm^{-1} can be assigned to the O–H stretch, and the 1608 cm^{-1} peak can be assigned to the H–O–H bending mode, respectively (30). As would be expected, these water-related peaks decrease in intensity by raising the temperature. A more interesting observation is the change of the relative peak intensities of the CN vibrational modes. The peak at 2162 cm^{-1} (Fe^{III}–CN–Co^{II}) decreased, and that at 2117 cm^{-1} (Fe^{II}–CN–Co^{III}) increased gradually by increasing the temperature. The former peak disappeared above 363 K, but a new peak at ~ 2080 cm^{-1} appeared above 333 K. These results show that dehydration first increases the fraction of Fe^{II}–CN–Co^{III}, indicating a CT from Co^{II} to Fe^{III}. Further dehydration destroys the ordered structure of the compound, as shown by DTA and XRD. It is, therefore, expected that the ν(CN) peak at ~ 2082 cm^{-1} corresponds to CN in the disordered structure.

This dehydration-induced charge transfer is supported by Mössbauer measurements. The spectrum of the compound dehydrated at 333 K is shown in Fig. 9. A fitting of the spectrum gives four pairs of doublets. The doublet (2) with $IS = -0.19$, $QS = 1.78$ and the doublet (4) with $IS = -0.09$, $QS = 0.72$ can be assigned to Fe^{III} and Fe^{II} respectively as described before. The doublet (3) with $IS = -0.05$ and $QS = 1.44$ has a similar IS value as doublet (4), indicating that the charge density of the iron responding for this doublet is close to that of the iron responding for the doublet (4). In contrast, the QS value of the doublet (3) is larger than that of the doublet (4), indicating that the symmetry is lower for the iron responsible for doublet (3) than that for doublet (4) (52, 53). Thus, the iron corresponding to the doublet (4) should be Fe^{II} with a lower symmetry, which

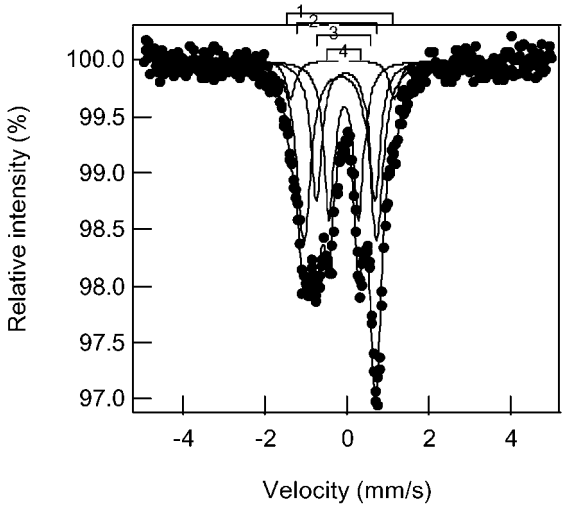

FIG. 9. Mössbauer spectrum of $CoFe(CN)_5NH_3 \cdot 6H_2O$ dehydrated at 333 K.

is a result of the shrinking of the lattice caused by dehydration. The doublet (1) with $IS = -0.13$ and $QS = 2.55$ may originate from the iron in a disordered or broken structure. The decrease in the ratio of Fe^{III} to the total Fe^{III} is about 37%. This result agrees with the change in the IR spectrum, which shows the ν(CN) in Fe^{III}–CN–Co^{II} decreases by about 38%.

The dehydration-induced changes in the fractions of Fe^{III}–CN–Co^{II} and Fe^{II}–CN–Co^{III} can also be observed in the UV-visible spectra. The spectrum of the compound before dehydration (Fig. 10, curve a) exhibits broad absorption in the near-IR region, which is always observed for aqua cobalt(II) compounds and is assigned to a *d–d*

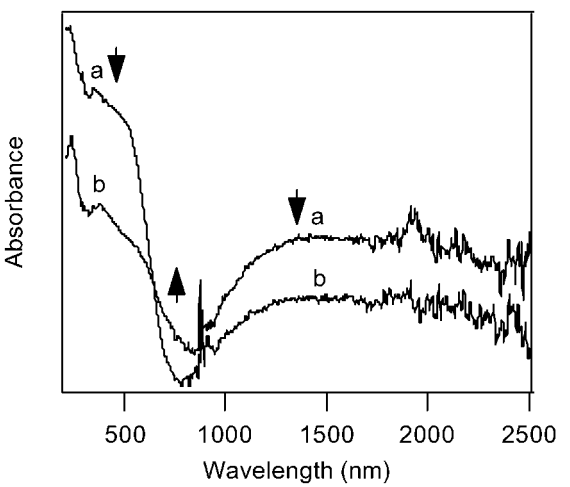

FIG. 10. Changes in the UV-visible spectrum induced by dehydration: (a) before and (b) after dehydration at 333 K.

transition. The CT band for Fe^{III}–CN–Co^{II} should also appear in this region. Conversely, for the Fe^{II}–CN–Co^{III} system, both the CT and *d–d* bands have peak positions in the range 500–800 nm (54, 55). In fact, the dehydration at 333 K decreased the broad absorption in the near IR region but increased the absorption in the range 650 to 850 nm, indicating a decrease in the Fe^{III}–CN–Co^{II} fraction and an increase in the Fe^{II}–CN–Co^{III} fraction (Fig. 10, curve b).

Apparently, the mechanism responsible for dehydration in the present case is different from that for $Co[Co(CN)_6]\cdot xH_2O$ (38). Variation in the coordination of the interstitial ions is the reason for the former but the change in the metal-cyanide network is the reason for the latter. As was previously described, dehydration below 340 K decreases the lattice constant while retaining the fcc structure. Because the change in the cobalt–iron–cyanide network derives mainly from the change in the N–Co bond length (18, 51), the present data suggest that the N–Co bond length decreases after dehydration. This change would increase the energy splitting between the e_g and t_{2g} orbitals (51). Because Co^{II} is in the high-spin state, the energy increase destabilizes the electrons in the e_g orbitals. As a result, these electrons are transferred to the low-lying t_{2g} orbitals of iron and cobalt, producing a stable Fe^{II}–CN–Co^{III} state. Fe^{III} is low spin ($S = \frac{1}{2}$) and Co^{II} is high spin ($S = \frac{3}{2}$) in Fe^{III}–CN–Co^{II}, while the low-spin states of Fe^{II} ($S = 0$) and Co^{III} ($S = 0$) may be the stable state in Fe^{II}–CN–Co^{III}. In other words, the spin number of the compound decreases as a result of dehydration, which is confirmed by the magnetic measurements.

Specifically, the temperature dependence of the effective magnetic moment (μ_{eff}) calculated from the χ value supports the spin number change due to dehydration. As shown in Fig. 11, although μ_{eff} was almost constant ($\sim 5.2\ \mu_B$) around 280 K, it gradually decreased as the temperature was raised and reached $\sim 4.4\ \mu_B$ at 337 K. These data agree with the electronic structural changes discussed above and further support the decrease of spin number. The μ_{eff} value increased slightly again above 337 K. When the compound was dehydrated at this temperature, the FCM did not increase even when the temperature was lowered to 2 K, as shown in Fig. 4 (curve d), indicating that the compound had converted to a paramagnetic state. Because 337 K is almost the same temperature where the DTA begins to increase (Fig. 8), the increase of μ_{eff} above this temperature is ascribed to the decomposition of the fcc crystal structure, probably to a material with uncoordinated cobalt ions.

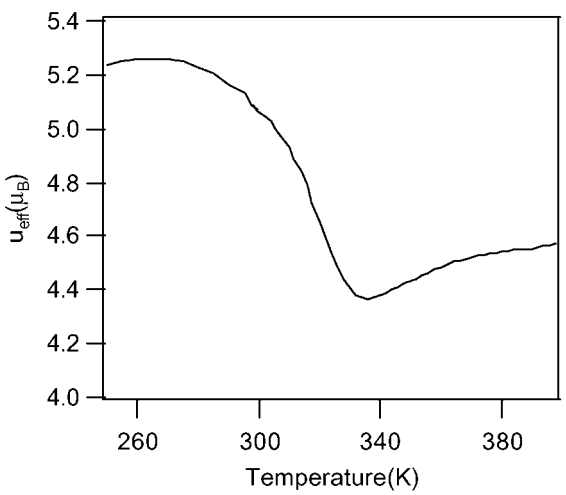

FIG. 11. Change of effective moment with increasing temperature.

CONCLUSIONS

We have shown that the Fe^{II}–CN–Co^{III} and Fe^{III}–CN–Co^{II} electronic structures coexist in $CoFe(CN)_5NH_3\cdot 6H_2O$. The photo-irradiation transfers electrons from Fe^{II} to Co^{III}, increasing the Fe^{III}–CN–Co^{II} population. As a result, the spontaneous magnetization increases. Conversely, the removal of uncoordinated water molecules in this compound decreased the fraction of the Fe^{III}–CN–Co^{II} state. These observations suggest that the potential energy surfaces for the Fe^{II}–CN–Co^{III} and Fe^{III}–CN–Co^{II} electronic structures are nearly degenerate, and thus these two configurations can interconvert as a result of a small perturbation.

REFERENCES

1. J. S. Miller and A. J. Epstein, *C&EN* **Oct. 2,** 30 (1995).
2. J. S. Miller and A. J. Epstein, *Angew. Chem. Int. Ed. Engl.* **33,** 385 (1994).
3. O. Kahn, "Molecular Magnetism." VCH, New York, 1993.
4. D. Gatteschi, O. Kahn, J. S. Miller, and F. Palacio, "Magnetic Molecular Materials." Kluwer, Dordrecht, Netherlands, 1991.
5. O. Kahn, *Nature* **378,** 667 (1995).
6. S. Ferlay, T. Mallah, R. Ouahes, P. Veillet, and M. Verdaguer, *Nature* **378,** 701 (1995).
7. W. R. Entley and G. S. Girolami, *Science* **268,** 397 (1995).
8. T. Mallah, S. Thiebaut, M. Verdaguer, and P. Veillet, *Science* **262,** 1554 (1993).
9. O. Sato, T. Iyoda, A. Fujishima, and K. Hashimoto, *Science* **272,** 704 (1996).
10. O. Sato, Y. Einaga, T. Iyoda, A. Fujishima, and K. Hashimoto, *J. Phys. Chem.* **101,** 3903 (1997).
11. M. Verdaguer, *Science* **272,** 698 (1996).
12. O. Sato, T. Iyoda, A. Fujishima, and K. Hashimoto, *Science* **271,** 49 (1996).
13. O. Sato, Y. Einaga, T. Iyoda, A. Fujishima, and K. Hashimoto, *J. Electrochem. Soc.* **11,** 144 (1997).
14. O. Sato, Y. Einaga, A. Fujishima, and K. Hashimoto, *Inorg. Chem.* **38,** 4405 (1999).
15. Y. Einaga, O. Sato, T. Iyoda, Y. Kobayashi, F. Ambe, K. Hashimoto, and A. Fujishima, *Chem. Lett.* 289 (1997).
16. N. Shimamoto, S. Ohkoshi, O. Sato, and K. Hashimoto, *Mol. Cryl. Liq. Cryst.* **344,** 95 (2000).

17. T. Yokoyama, M. Kiguchi, T. Ohta, Y. Einaga, O. Sato, and K. Hashimoto, *Phys. Rev. B* **60,** 9340 (1999).
18. T. Yokoyama, T. Ohta, O. Sato, and K. Hashimoto, *Phys. Rev. B* **58,** 8287 (1998).
19. A. Bleuzen, C. Lomenech, A. Dolbecq, F. Villain, A. Goujon, O. Roubeau, M. Nogues, F. Varret, F. Baudelet, E. Dartyge, C. Giorgetti, J. J. Gallet, C. Cartier dit Moulin, and M. Verdaguer, *Mol. Cryst. Liq. Cryst.* **335,** 253 (1999).
20. A. Bleuzen, C. Lomenech, V. Escax, F. Villain, F. Varret, C. Cartier dit Moulin, and M. Verdaguer, *J. Am. Chem. Soc.* **122,** 6648 (2000).
21. C. Cartier dit Moulin, F. Villain, A. Bleuzen, C. Lomenech, M. A. Arrio, P. Sainctavit, C. Lomenech, V. Escax, F. Baudelet, E. Dartyge, J. J. Gallet, and M. Verdaguer, *J. Am. Chem. Soc.* **122,** 6653 (2000).
22. D. A. Pejakovic, J. L. Manson, J. S. Miller, and A. J. Epstein, *Phys. Rev. Lett.* **85,** 1994 (2000).
23. M. Nishino and K. Yamaguchi, *Phys. Rev. B* **58,** 9303 (1998).
24. T. Kawamoto, Y. Asai, and S. Abe, *Phys. Rev. B* **60,** 12990 (1999).
25. K. Yoshizawa, F. Mohri, G. Nuspl, and T. Yamabe, *J. Phys. Chem. B* **102,** 5432 (1998).
26. E. Fluck, H. Inoue, M. Nagao, and Y. Yanagisawa, *J. Inorg. Nucl. Chem.* **41,** 287 (1979).
27. E. Reguera, J. Fernandez-Bertran, and A. Gomez, *Eur. J. Solid State Inorg. Chem.* **31,** 979 (1994).
28. D. F. Mullica, E. L. Sappenfield, D. B. Tippin, and D. H. Leschnitzer, *Inorg. Chim. Acta* **164,** 99 (1989).
29. D. F. Mullica, D. B. Tippin, and E. L. Sappenfield, *Inorg. Chim. Acta* **174,** 129 (1990).
30. D. F. Mullica, D. B. Tippin, and E. L. Sappenfield, *J. Coord. Chem.* **24,** 83 (1991).
31. D. F. Mullica, D. B. Tippin, and E. L. Sappenfield, *J. Cryst. Spectrosc. Res.* **21,** 81 (1991).
32. S. Turner, O. Kahn, and L. Rabardel, *J. Am. Chem. Soc.* **118,** 6428 (1996).
33. K. Nakatani, P. Bergerat, E. Codjovi, C. Mathoniere, Y. Pei, and O. Kahn, *Inorg. Chem.* **30,** 3977 (1991).
34. K. V. Langenberg, S. R. Batten, K. J. Berry, D. C. R. Hockless, B. Moubaraki, and K. S. Murray, *Inorg. Chem.* **36,** 5006 (1997).
35. J. Larionova, S. A. Chavan, J. V. Yakhmi, A. G. Froystein, J. Sletten, C. Sourisseau, and O. Kahn, *Inorg. Chem.* **36,** 6374 (1997).
36. N. Re, R. Crescenzi, C. Floriani, H. Miyasaka, and N. Matsumoto, *Inorg. Chem.* **37,** 2717 (1998).
37. J. Larionova, R. Clerac, J. Sanchiz, O. Kahn, S. Golhen, and L. Ouahab, *J. Am. Chem. Soc.* **120,** 13,088 (1998).
38. D. F. Shriver and D. B. Brown, *Inorg. Chem.* **8,** 42 (1969).
39. L. A. Gentil, E. J. Baran, and P. J. Aymonino, *Inorg. Chim. Acta* **20,** 251 (1976).
40. G. Brauer, "Prep. Inorg. Chem.," p. 1512. Academic Press, New York, 1963.
41. K. A. Hofmann, *Ann.* **312,** 24 (1900).
42. F. Holzl and K. Rokitasky, *Monatsh. Chem.* **56,** 82 (1930).
43. H. J. Buser, D. Schwarzenbach, W. Petter, and A. Ludi, *Inorg. Chem.* **16,** 2704 (1977).
44. D. B. Brown and S. F. Shriver, *Inorg. Chem.* **8,** 37 (1969).
45. Z.-Z. Gu, O. Sato, T. Iyoda, K. Hashimoto, and A. Fujishima, *Chem. Mater.* **9,** 1092 (1997).
46. K. Nakamoto, "Infrared and Raman Spectra of Inorganic and Coordination Compounds." Wiley–Interscience, New York, 1986.
47. C. R. Johnson and R. E. Shepherd, *Inorg. Chem.* **22,** 3506 (1983).
48. T. K. McNab, H. Micklitz, and P. H. BarreH, in "Mossbauer Isomer Shifts" (G. K. Shenoy and E. E. Wagner, Eds.). North-Holland, Amsterdam, 1978.
49. Y. Einaga, Z.-Z. Gu, O. Sato, T. Iyoda, K. Hashimoto, and A. Fujishima, *Hyper. Interact.* **116,** 159 (1998).
50. B. N. Figgis, "Introduction to Ligand Fields." Interscience, New York.
51. Z.-Z. Gu, Thesis, University of Tokyo, Tokyo, 1998.
52. H. Frauenfelder, "Mossbauer Effect." W. A. Benjamin, New York, 1963.
53. V. I. Gol'danskii and R. H. Herber, "Chemical Applications of Mossbauer Spectroscopy." Academic Press, New York, 1968.
54. S. Bagger and P. Stoltze, *Acta Chem. Scand. A* **35,** 509 (1981).
55. A. Vogler and H. Kunkely, *Ber. Bunsen-Ges. Phys. Chem.* **79,** 83 (1975).